Shands, K. M., Schmid, G. P., Dan, B. B., Blum, D., Guidotti, R. J., Hargrett, M. T., Anderson, R. L., Hill, D. L., Broome, C. V., Band, J. D., & Fraser, D. W. (1980) *N. Engl. J. Med. 303*, 1436–1442.

Singh, B. R., Evenson, M. L., & Bergdoll, M. S. (1988) *Biochemistry* (following paper in this issue).

Stern, O., & Volmer, M. (1919) *Phys. Z. 20*, 183–188.

Teale, F. W., & Weber, G. (1957) *Biochem. J. 65*, 476–482.

Structural Analysis of Staphylococcal Enterotoxins B and C_1 Using Circular Dichroism and Fluorescence Spectroscopy†

Bal Ram Singh, Mary L. Evenson, and Merlin S. Bergdoll*

Food Research Institute, University of Wisconsin—Madison, Madison, Wisconsin 53706

Received April 1, 1988; Revised Manuscript Received July 8, 1988

ABSTRACT: Secondary and tertiary structural parameters of two functionally and serologically related proteins, staphylococcal enterotoxins B and C_1, have been determined by using circular dichroism and fluorescence spectroscopy. The secondary structures derived from the respective far-UV circular dichroic spectra were 9.5% α-helix, 55.0% β-pleated sheets, 16.5% β-turns, and 19.0% random coils for enterotoxin B and 15.0% α-helix, 38.0% β-pleated sheets, 25.5% β-turns, and 21.5% random coils for staphylococcal enterotoxin C_1. The values matched well with the secondary structures derived from the amino acid sequences (Chou and Fasman method). Seven antigenic sites have been predicted for both staphylococcal enterotoxins B and C_1 by using the hydrophilicity and the secondary structure information. Three of these antigenic sites appear similar. Fluorescence quantum yield of the single tryptophan residue (Trp-197) of both the enterotoxins showed the tryptophan residue in staphylococcal enterotoxin B to be ~46% more fluorescent than in staphylococcal enterotoxin C_1. Tryptophan fluorescence quenching by the surface quencher I^- and the neutral quencher acrylamide revealed that the single tryptophan residue in each of the enterotoxins is buried in the protein matrix and is not accessible to the surface quencher I^-. The tryptophan residue in staphylococcal enterotoxin C_1 is 14% less accessible to acrylamide than in staphylococcal enterotoxin B. The data, in general, reflect several similarities and significant differences between the two related enterotoxins.

The staphylococcal enterotoxins are a group of toxins that is responsible for bacterial food poisoning resulting in diarrhea and emesis. Staphylococcal enterotoxins B (SEB) and C_1 (SEC_1) have 239 amino acids each with molecular weights of 28.4K and 27.5K, respectively (Huang & Bergdoll, 1970; Schmidt & Spero, 1983). SEB and SEC_1 have significant serological cross-reactivity (Johnson et al., 1972; Spero et al., 1978) and a sequence homology of about 65% (Schmidt & Spero, 1983). Both toxins have a similar level of toxicity (Bergdoll, 1983). Clearly, a 35% difference in the amino acid sequence does not affect the biological activity of the toxins. Moreover, SEB and SEC_1 have significant differences in the nature of amino acids in their composition; SEB contains both more hydrophobic and more charged amino acids than SEC_1 (Huang & Bergdoll, 1970; Schmidt & Spero, 1983).

In order to establish a structural basis for their common biological action, secondary structure parameters for SEB and SEC_1 are derived from their respective far-UV circular dichroic (CD) spectra and compared with the predicted secondary structures based on the primary structure (Chou & Fasman, 1978). Probable antigenic sites are predicted by using the secondary structure information in conjunction with hydrophilicity. Secondary structures of SEB and SEC_1 were analyzed by Middlebrook et al. (1980). However, data were analyzed only for α-helices based on crude methods of Greenfield and Fasman (1969) and Chen et al. (1972). In this study, secondary structures were determined from the far-UV CD spectra by using the method of Chang et al. (1978) for α-helix, β-pleated sheets, β-turns, and random coils. In this method, the secondary structures are derived from a linear least-squares fit of the far-UV CD spectra of 15 reference proteins of known secondary structures.

Both SEB and SEC_1 have single tryptophan residues in their primary structure (Huang & Bergdoll, 1970; Schmidt & Spero, 1983) which are located at identical positions. This system is ideal for probing the topography of these tryptophan residues. Any differences in the microenvironments of the tryptophan residues should reflect differences in the protein folding (tertiary structure). Intrinsic fluorescence spectroscopy has been utilized to detect any differences in the surroundings of the single tryptophan residue each in SEB and SEC_1.

Materials and Methods

Materials. SEB and SEC_1 were purified and stored as lyophilized powders at 4 °C (Schantz et al., 1965; Borja & Bergdoll, 1967). Toxins were dissolved in 10 mM sodium phosphate buffer (NaPB), pH 7.2, just before use, and the protein solutions were filtered through 0.2-μm filters (Millipore) to get optically clear solutions. All the chemicals used were of the highest grade commercially available, and solutions and buffers were made with distilled water.

Absorption Spectra. Absorption measurements were made on a DU-7 spectrophotometer (Beckman Instruments). Far-UV circular dichroic spectra were recorded on a JASCO

† This work was supported in part by NIH Grant NS 17742 and DOD–University Research Instrumentation Award DAAG-29-83-G0063 to B. R. DasGupta and by the College of Agricultural and Life Sciences, University of Wisconsin–Madison.

* Address correspondence to this author.

0006-2960/88/0427-8735$01.50/0

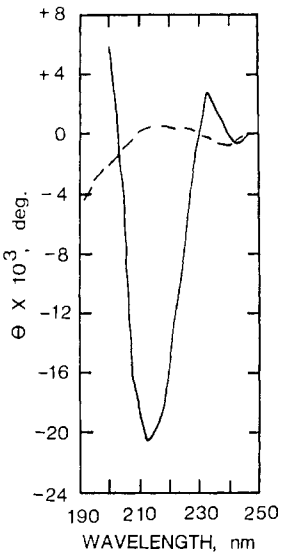

FIGURE 1: Far-UV CD spectrum (solid line) of SEB dissolved in 10 mM NaPB, pH 7.2. The concentration of SEB was 0.49 mg/mL, and the spectrum was recorded by using a 1-mm path-length cuvette at room temperature (23–25 °C). The dashed line is the base line recorded for 10 mM NaPB, pH 7.2.

J-20A CD/ORD spectropolarimeter at room temperature (23–25 °C) with a chart speed of 2 cm/min and a wavelength expansion of 10 nm/cm. The slit width and the time constant were fixed at 1 nm and 4 s, respectively. The spectra were recorded using a 1-mm path-length quartz cuvette with protein concentrations of 0.5–0.6 mg/mL. Mean residue ellipticities were calculated between 195 and 240 nm at 1-nm intervals.

Fluorescence Spectra. Fluorescence spectra were recorded on an SLM 8000 "smart" spectrofluorometer, and the spectral processings were carried out by using a "spectrum processor PR 8002" provided by SLM Instruments. For the tryptophan fluorescence spectra, SEB and SEC_1 having an A_{295} of less than 0.1 were used to minimize the inner filter effect. An excitation wavelength of 295 nm was used in order to preferentially excite the tryptophan residues. Emission spectra were recorded at room temperature (23–25 °C) between 310 and 410 nm with excitation and emission resolutions of 2 and 4 nm, respectively. Tryptophan fluorescence quantum yields were determined by calculating the area under the emission spectra of SEB, SEC_1, and free L-tryptophan (all having the same A_{295}) between 310 and 410 nm and by comparing these values with the published fluorescence quantum yield of free L-tryptophan (Teale & Weber, 1957).

For fluorescence quenching experiments, stock solutions of KI (5 M) and acrylamide (8 M) were prepared. Small amounts of the stock solutions were added stepwise (total of 20–25 μL) to 700 μL of SEB and SEC_1 and the spectra recorded. Fluorescence intensity at the λ_{max} was used for the analysis of data for Stern–Volmer plots (Stern & Volmer, 1919):

$$F_0/F = 1 + K_{sv}[Q] \quad (1)$$

where F_0 and F are the fluorescence intensities in the absence and presence of a given concentration of a given quencher, [Q]. K_{sv} is the Stern–Volmer constant. The data were also analyzed for the modified Stern–Volmer plots (Lehrer, 1971):

$$F_0/\Delta F = 1/f_{acc} + 1/f_{acc}K_Q[Q] \quad (2)$$

where ΔF is the difference in the fluorescence intensity after the addition of a given concentration of a quencher, f_{acc} is the fraction of maximum accessible tryptophan fluorescence, and K_Q is the effective quenching constant.

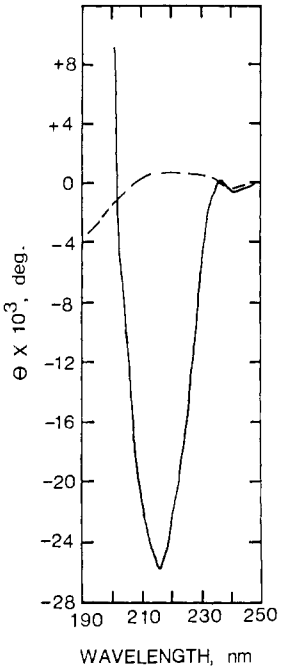

FIGURE 2: Far-UV CD spectrum (solid line) of SEC_1 dissolved in 10 mM NaPB, pH 7.2. The concentration of SEC_1 was 0.64 mg/mL. The dashed line is the base line recorded for 10 mM NaPB, pH 7.2. Other conditions were the same as in Figure 1.

Table I: Secondary Structure Analysis of SEB and SEC_1 Derived from Their Respective Far-UV CD Spectra and the Amino Acid (aa) Sequences

	SEB		SEC_1	
secondary structure	CD	aa sequence	CD	aa sequence
% α-helix	9.5	14.4	15.0	20.8
% β-pleated sheets	55.0	21.6	38.0	17.4
% β-turns	16.5	54.2	25.5	53.0
% random coils	19.0	9.7	21.5	8.9

Since acrylamide absorbs significantly at 295 nm (molar absorption extinction coefficient was determined to be 0.266 M^{-1} cm^{-1} in the protein solution dissolved in 10 mM NaPB, pH 7.5), the fluorescence intensity was corrected according to Eftink and Ghiron (1976).

RESULTS

Secondary Structure. Secondary structure parameters were derived from the far-UV CD spectra of SEB and SEC_1 dissolved in 10 mM NaPB, pH 7.5. The CD spectra of SEB and SEC_1 are shown in Figures 1 and 2, respectively. Both spectra show single-well structures with negative maxima at ~215 nm. Such spectra are indicative of predominantly β-pleated sheets in the secondary structure of the proteins (Cantor & Schimmel, 1980). It is noteworthy that SEB shows a small positive CD band at 233 nm (Figure 1) which is absent in SEC_1 (Figure 2). Mean residue ellipticities at the negative maximum were very similar for SEB (−5103 deg·cm^2 $dmol^{-1}$ at 214 nm) and SEC_1 (−4763 deg·cm^2 $dmol^{-1}$ at 216 nm). Secondary structure calculations showed 9.5% α-helix, 55.0% β-pleated sheets, 16.5% β-turns, and 19.0% random coils for SEB (Table I) and 15.0% α-helix, 38.0% β-pleated sheets, 25.5% β-turns, and 21.5% random coils for SEC_1. These two enterotoxins have similar secondary structures with low α-helical content. However, SEC_1 appears to have significantly more α-helix than SEB. The increase in the α-helix is mainly at the expense of β-pleated sheets (Table I). The secondary structure parameters calculated from the primary structure by the method of Chou and Fasman (1978) using a program

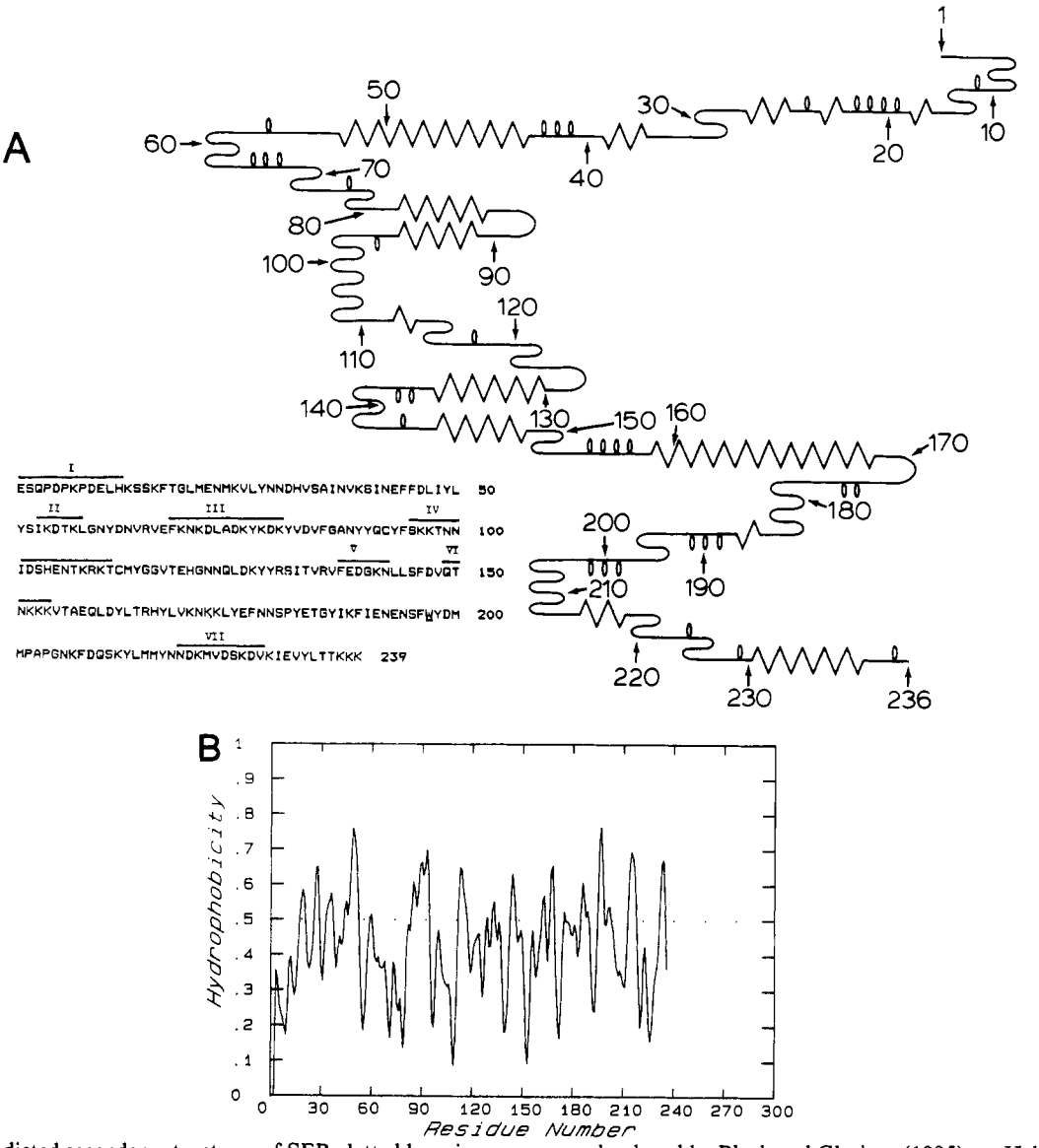

FIGURE 3: (A) Predicted secondary structures of SEB plotted by using a program developed by Black and Glorioso (1985). α-Helix, β-sheets, β-turns, and random coils are represented by looped, jagged, wavy, and solid lines, respectively. The amino acid sequence of SEB (Huang & Bergdoll, 1970) is shown also. The overlines with Roman numerals represent the predicted antigenic determinants. (B) Zero-order hydrophobicity (inverted hydrophilicity) profiles of SEB using the parameters of Hopp and Woods (1982) with a running window of five amino acid residues. Parameters are scaled to the range 0–1 where 0 is the most hydrophilic (polar) and 1 is the most hydrophobic. The original hydrophilicity parameters (Y) can be obtained by using the equation $Y = (X - 0.46875)/0.15625$ where X is the scale on the y axis of the plot.

(Black & Glorioso, 1985) show 14.4% and 20.8% α-helix, 21.6% and 17.4% β-pleated sheets, 54.2% and 53.0% β-turns, and 9.7% and 8.9% random coils, respectively, for SEB and SEC_1. The predicted secondary structures also show similar patterns for both proteins. The β-pleated sheets and β-turns predicted from the amino acid sequences do not match with the parameters determined by the circular dichroic spectroscopy. However, the combined amount of β-pleated sheets and β-turns matches well with the experimentally derived contents. The discrepancy could be due to the inherent inaccuracies in the programs used for the analyses. The method of Chang et al. (1978) is especially weak in the determination of β-turns, but such a high amount of β-turns as predicted by the Chou and Fasman method is not likely for these small proteins.

Antigenic Determinants. The antigenic determinants were predicted according to the method of Hopp and Woods (1982) with a running window of five amino acid residues. Seven probable antigenic determinants were predicted for both SEB and SEC_1 having a hydrophilicity range of 1.51–2.44 (Figures 3B and 4B). Almost all of the predicted antigenic determinants had β-turns in their secondary structure, making them more likely to be antigenic sites. The antigenic determinants represented by their amino acid sequences and corresponding secondary structures are shown in Figures 3A and 4A for SEB and SEC_1, respectively. The predicted sites are arbitrarily classified into strong, moderate, and weak depending on their hydrophilicity. A site having a hydrophilicity of more than 2.4 is considered strong, more than 2.0 is moderate, and more than 1.5 is weak. Out of seven antigenic sites in SEB, two make very strong antigenic determinants (minimum hydrophilicity $\sim$2.4), and two are moderate, and the other three are weak antigenic determinants. In the case of SEC_1, only one site is predicted to be a strong antigenic determinant, two are moderate, and the other four are weak. Three of the antigenic sites (I, VI, and VII; Figures 3 and 4) appear to be similar in SEB and SEC_1; the rest appear different.

Fluorescence Spectroscopy. Fluorescence spectra (Figure 5) of both SEB and SEC_1 show emission maxima at 333 nm (excitation at 295 nm). The tryptophan fluorescence quantum yield revealed that the single tryptophan residue in SEB is

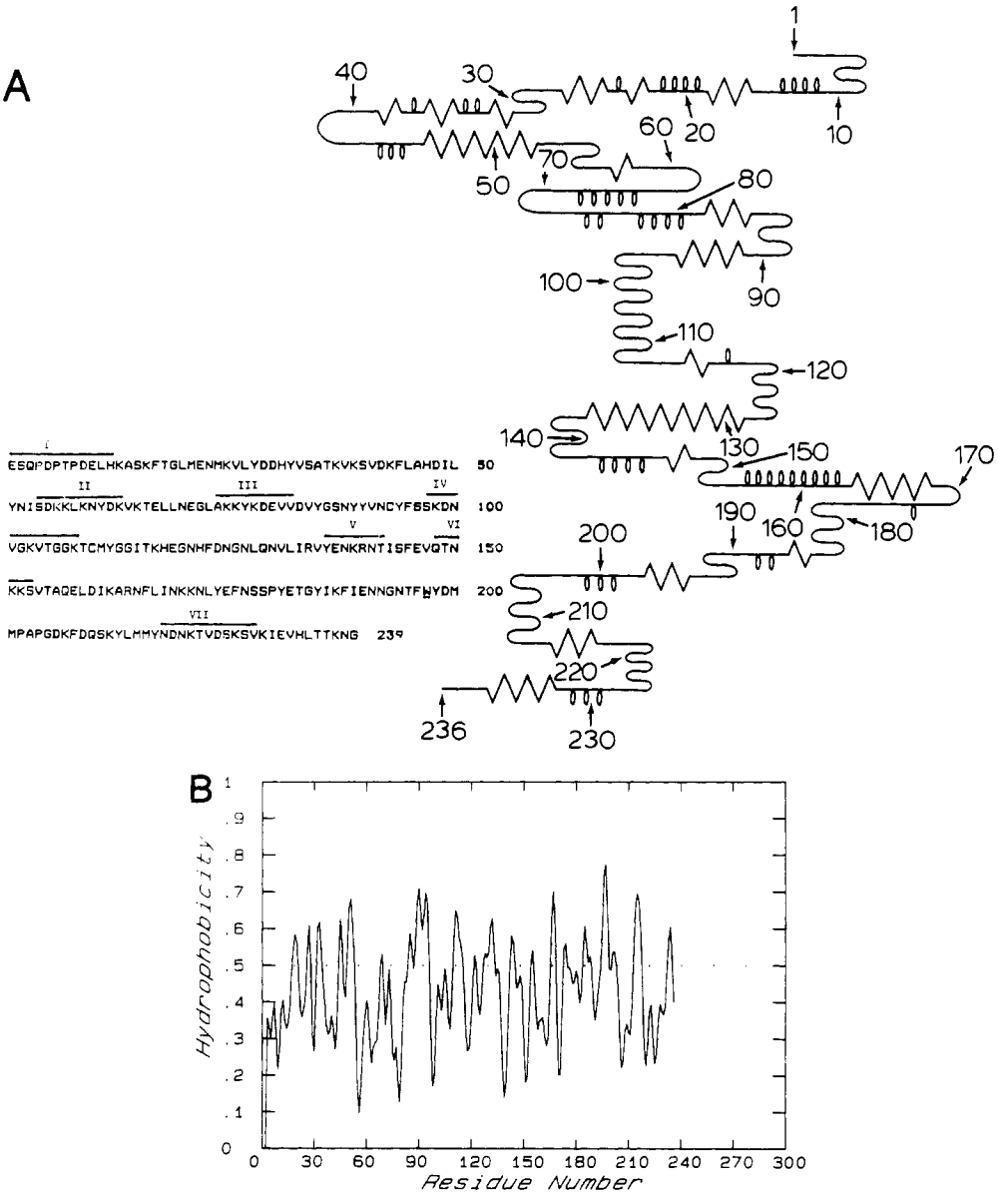

FIGURE 4: Predicted secondary structures of SEC_1 plotted by using a program developed by Black and Glorioso (1985). For symbols, see Figure 3A. The amino acid sequence of SEC_1 (Schmidt & Spero, 1983) is shown also. The overlines with Roman numerals represent the predicted antigenic determinants. (B) Zero-order hydrophobicity (inverted hydrophilicity) profile of SEC_1 using the parameters of Hopp and Woods (1982) with a running window of five amino acid residues. For other details, see Figure 3B.

Table II: Tryptophan Fluorescence Characteristics of SEB and SEC_1

enterotoxin	emission maximum (nm)	tryptophan fluorescence quantum yield
SEB	333 ± 1	0.28
SEC_1	333 ± 1	0.19

about 46% more fluorescent than that in SEC_1 (Table II), indicating that the surroundings of the tryptophan residues are significantly different in the two related toxins.

The microenvironment of the single tryptophan residue in SEB and SEC_1 is further investigated by using a surface quencher (I^-) and a neutral (hydrophobic) quencher (acrylamide). A representative set of fluorescence spectra showing quenching by acrylamide is shown in Figure 6. The Stern–Volmer plots for tryptophan fluorescence quenching by I^- and acrylamide in SEB are shown in Figure 7. The K_{sv} values for the tryptophan fluorescence quenching were 0.00 and 4.41 M^{-1} for I^- and acrylamide, respectively (Table III). The Stern–Volmer analysis (Figure 8) of the tryptophan fluorescence quenching in SEC_1 revealed K_{sv} values of 0.25 and 4.23 M^{-1}, respectively, for I^- and acrylamide quenching (Table III). The modified Stern–Volmer plots for acrylamide quenching of the tryptophan fluorescence in SEB and SEC_1 are shown in Figure 9. The fraction of maximum tryptophan fluorescence accessible to acrylamide was quite high for both SEB and SEC_1 (1.00 and 0.86, respectively; Table III).

Table III: Tryptophan Fluorescence Quenching Parameters[a] for SEB and SEC_1

	I^-			acrylamide		
enterotoxin	K_{sv}	K_Q	f_{acc}	K_{sv}	k_Q	f_{acc}
SEB	0.00			4.41	4.53	1.00
SEC_1	0.25			4.23	5.86	0.86

[a] Units of the quenching parameters are expressed as follows: K_{sv}, M^{-1}; K_Q, M^{-1}; f_{acc}, fraction.

DISCUSSION

There are seven serologically distinguishable staphylococcal enterotoxins which have similar biological activities (Bergdoll,

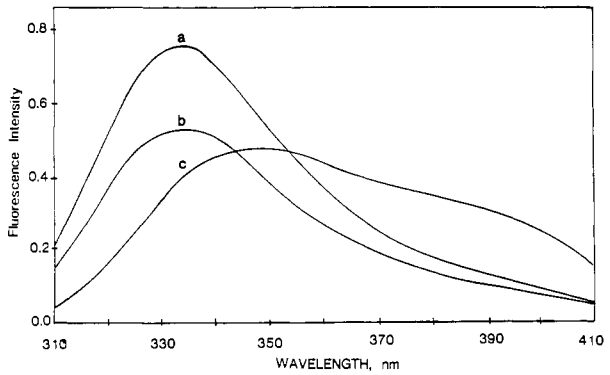

FIGURE 5: Tryptophan fluorescence spectra of (a) SEB, (b) SEC_1, and (c) free L-tryptophan dissolved in 10 mM NaPB, pH 7.2. Excitation wavelength was 295 nm, and spectral resolutions of excitation and emission monochromators were 2 and 4 nm, respectively. Absorbance at 295 nm (excitation wavelength) was 0.055, 0.053, and 0.057, respectively, for SEB, SEC_1, and free L-tryptophan. All the recordings were carried out at room temperature (23–25 °C).

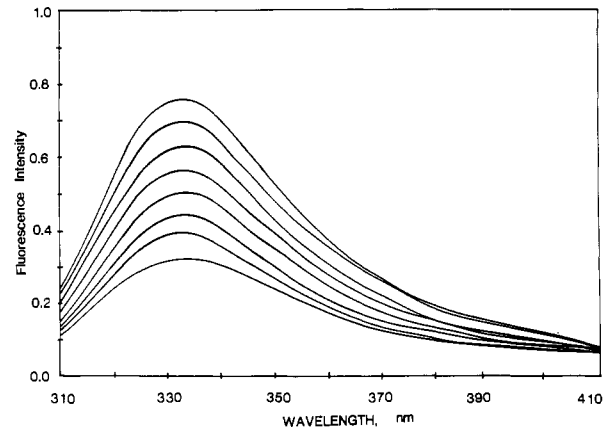

FIGURE 6: Tryptophan fluorescence spectra of SEB dissolved in 10 mM NaPB, pH 7.2, after mixing with different concentrations of acrylamide. The concentrations of acrylamide used were 0 (top spectrum), 0.015, 0.043, 0.072, 0.101, 0.143, 0.185, and 0.24 M (bottom spectrum). Other conditions were the same as in Figure 5.

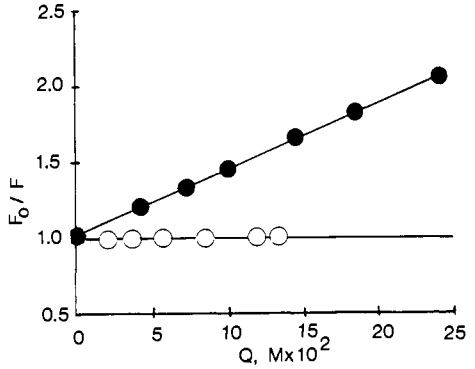

FIGURE 7: Stern–Volmer plots for I^- (open circles) and acrylamide (closed circles) quenching of the tryptophan fluorescence in SEB. F_0 is the fluorescence intensity in the absence of quencher, and F is the fluorescence intensity in the presence of a given concentration of the quencher, Q. Fluorescence spectra were recorded under the same conditions as in Figures 5 and 6.

1983). It is not understood how these enterotoxins having sequence homologies as low as 30% and as high as 86% have similar biological activities but different antigenic determinants. In other words, the structural basis of the biological functions and the serological reactivity is not well understood. Furthermore, the molecular mechanism of the toxin action is also not known. The structural analysis of two closely related staphylococcal enterotoxins (B and C_1) is aimed at providing

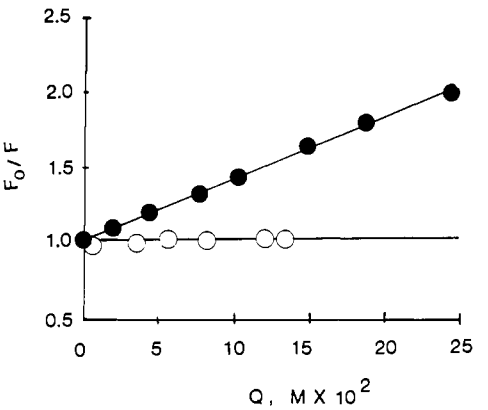

FIGURE 8: Stern–Volmer plots for I^- (open circles) and acrylamide (closed circles) quenching of the tryptophan fluorescence in SEC_1. For symbols and spectral recording conditions, see Figure 7.

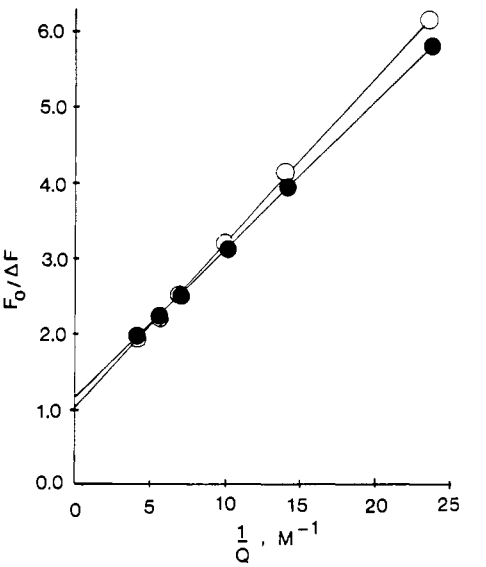

FIGURE 9: Modified Stern–Volmer plots of acrylamide quenching of the tryptophan fluorescence in SEB (open circles) and SEC_1 (closed circles). F_0 is the fluorescence intensity in the absence of quencher, and ΔF is the difference in the fluorescence intensity after mixing the protein with a given concentration of quencher, Q. For the conditions of spectral recordings, see Figure 6.

the structural basis of the differences in their serological properties and the similarities in their biological function.

Secondary structures of both SEB and SEC_1 have similar patterns (predominantly β-pleated sheets/β-turn structures; Table I). The small positive CD peak at 233 nm in SEB indicates the presence of more β-sheet compared to SEC_1. Certain proteins in the β-sheet conformation show a positive CD signal between 230 and 240 nm (Saxena & Wetlaufer, 1971). This is consistent with the secondary structure calculations (Table I). The CD signal at ≈230 nm also could arise due to aromatic amino acids, especially tyrosine (Beychok, 1966; Bewley et al., 1972), but such a possibility is unlikely as no major differences were found in the near-UV CD of SEB and SEC_1 (Spero, 1981). The pattern of secondary structure in SEB and SEC_1 is the same as that for enterotoxins A (SEA) and E (SEE) (B. R. Singh and M. J. Betley, unpublished results). SEA and SEE have very low sequence homology with either SEB or SEC_1 [see Betley & Mekalanos (1988)]. The role of high β-pleated sheets/β-turns cannot be ascertained at this point unless the basic mechanism of their action is understood. In any case, it seems that a high content of β-pleated sheets is maintained in all the staphylococcal enterotoxins and even in toxic-shock syndrome toxin 1 (Singh

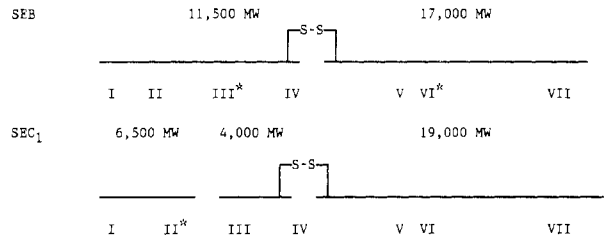

FIGURE 10: Schematic diagrams of SEB and SEC_1 showing antigenic sites (Roman numerals). Tryptic cleavage sites are represented by gaps in the lines. Asterisks identify strong antigenic sites. Sites I, VI, and VII have very similar amino acid sequences.

et al., 1988), also produced by *Staphylococcus aureus*.

Antigenic sites, as predicted by high hydrophilicity, indicate that such sites are spread over the sequence of both SEB and SEC_1 (Figures 3 and 4). There are two strong antigenic sites in SEB (residues 95–111 and 149–154) whereas in SEC_1 only one strong antigenic site was predicted (residues 54–63, Figure 10). The strong antigenic site in SEC_1 falls in the region of a cleavage site for trypsin, indicating that the site is accessible to exogenous proteins. However, the corresponding site in SEB (residues 54–63) has low hydrophilicity. One of the strong antigenic sites of SEB (residues 149–154) has very strong similarity with a predicted weak antigenic site in SEC_1 (QTNKK*K*VTA in SEB vs QTNKK*S*VTA in SEC_1), differing only in one amino acid residue.

It is interesting to note that the disulfide bond loop is a strong antigenic site in SEB (residues 95–111) but not as strong in SEC_1 (residues 97–108). Even though the predicted secondary structures of the disulfide loops of SEB and SEC_1 are the same (β-turns), there is almost no similarity in their amino acid sequences. It has been suggested that the toxic site of these toxins is in or near the disulfide loop (Huang et al., 1975). The similarity of three out of seven predicted antigenic sites comes to about 43% theoretical cross-reactivity between SEB and SEC_1. This comes very close to the 33% observed cross-reactivity between them (Spero et al., 1978; Johnson et al., 1972). Experiments with monoclonal antibodies have revealed that at least two monoclonal antibodies raised against SEB and SEC_1 reacted with both enterotoxins and do not appear identical (Thompson et al., 1984). This supports the validity of the prediction of three antigenic sites on SEB and SEC_1 which may be responsible for the serological cross-reactivity. The observation of at least two antigenic sites on SEB (Spero & Morlock, 1979) agrees with the two strong sites predicted in this report. One of the two predicted strong determinants for SEB (residues 149–154) falls well within the 17 000 molecular weight carboxy-terminal fragment identified by Spero and Morlock (1979), and the other is near a tryptic cleavage site (residue 95–111). Other predicted antigenic determinants may be present but probably could not be detected with polyclonal antibodies since there were only two fragments created by trypsinization.

In the case of SEC_1, the strongest predicted antigenic determinant lies within the first 7.2 kDa (very close to the one observed to cross-react with polyclonal antiserum within the 6.5-kDa fragment; Spero & Morlock, 1978) and is near a cleavage site for trypsin. Thus, in general, the antigenic determinants are supported by the experimental observation and can be used reliably as specific antigenic sites.

SEB and SEC_1 are ideal for probing the environment of tryptophan residues for any differences. They both have only one tryptophan residue, and the surrounding amino acid residues of Trp-197 (both in SEB and in SEC_1) are identical in both the enterotoxins. Tryptophan fluorescence maxima of 333 nm in both SEB and SEC_1 are an indication of a relatively nonpolar surrounding of their respective tryptophan residues. However, there is ~46% difference in the tryptophan fluorescence quantum yield (Table II) of the two enterotoxins, suggesting a significant difference in the surrounding groups of the tryptophan residues. Amino acids are known to quench the indole fluorescence (Longworth, 1971; Bertolotti et al., 1987). Since the immediate surrounding amino acid residues of Trp-197 are identical in SEB and SEC_1 in their respective primary structure, the observed difference in the tryptophan fluorescence quantum yields reflects differences in surrounding amino acid residues due to the differential polypeptide folding.

Fluorescence quenching data suggest that the single tryptophan residue in SEB and SEC_1 is not exposed on the surface of the protein as I^-, a surface quencher, is not effective (low K_{sv}) in quenching the tryptophan fluorescence (Table III). In other words, the tryptophan residue is not accessible to I^-. Acrylamide quenching seems to be very effective in both SEB and SEC_1 with a K_{sv} of more than 4.2 M^{-1}. The accessibility of the Trp-197 is very high for acrylamide in both SEB and SEC_1 with about 14% more accessibility in SEB over SEC_1 (Table III). This observation further confirms the conclusion that the tryptophan residues in both SEB and SEC_1 are in a hydrophobic environment. Fluorescence quenching results also suggest that the tryptophan residues are buried deep inside the protein matrix as they are only accessible to the penetrating quencher acrylamide (Eftink & Ghiron, 1984) as opposed to the surface quencher I^-. This comparison is appropriate because I^- and acrylamide both have a quenching efficiency of unity and the observed differences are expected to arise from differential accessibility (Eftink & Ghiron, 1981).

In conclusion, the data presented above suggest (1) SEB and SEC_1 maintain a similar pattern of secondary structure irrespective of differences in their sequence, (2) there is a relatively low α-helix and high β-sheet content in SEB compared to SEC_1, (3) there are seven predicted antigenic determinants with about 40% of them similar between SEB and SEC_1, (4) the single tryptophan residue in SEB and SEC_1 is deeply buried in a hydrophobic matrix of their respective proteins, and (5) the polypeptide folding (tertiary structure) of SEB and SEC_1, as probed by the tryptophan fluorescence quantum yield and intrinsic fluorescence quenching, appears to be significantly different.

REFERENCES

Bergdoll, M. S. (1983) *Staphylococci and Staphylococcal Infections*, Vol. 2, pp 559–598, Academic, New York.

Bertolotti, S. G., Bohorquez, M. D. V., Cosa, J. J., Garcia, M. A., & Previtali, C. M. (1987) *Photochem. Photobiol. 46*, 331–335.

Betley, M. J., & Makalanos, J. J. (1988) *J. Bacteriol. 170*, 34–42.

Bewley, T. A., Sairam, M. R., & Li, C. H. (1972) *Biochemistry 11*, 932–936.

Beychok, S. (1966) *Science (Washington, D.C.) 154*, 1288–1299.

Black, S. D., & Glorioso, J. C. (1985) *BioTechniques 4*, 448–460.

Borja, C. R., & Bergdoll, M. S. (1967) *Biochemistry 6*, 1467–1473.

Cantor, C. R., & Schimmel, P. R. (1980) *Biophysical Chemistry (Part II). Techniques for the Study of Biological Structure and Function*, pp 409–432, W. H. Freeman, San Francisco.

Chang, T. C., Wu, C.-S. C., & Yang, J. T. (1978) *Anal. Biochem. 91*, 13–31.

Chen, Y. H., Yang, J. T., & Martinez, H. M. (1972) *Biochemistry 11*, 4120–4131.
Chou, P. Y., & Fasman, G. D. (1978) *Annu. Rev. Biochem. 47*, 251–276.
Eftink, M. R., & Ghiron, C. A. (1976) *J. Phys. Chem. 80*, 486–493.
Eftink, M. R., & Ghiron, C. A. (1981) *Anal. Biochem. 114*, 199–227.
Eftink, M. R., & Ghiron, C. A. (1984) *Biochemistry 23*, 3891–3899.
Greenfield, N., & Fasman, G. D. (1969) *Biochemistry 8*, 4108–4116.
Hopp, T. P., & Woods, K. R. (1982) *Proc. Natl. Acad. Sci. U.S.A. 78*, 3824–3828.
Huang, I.-Y., & Bergdoll, M. S. (1970) *J. Biol. Chem. 245*, 3518–3525.
Huang, I.-Y., Schantz, E. J., & Bergdoll, M. S. (1975) *Jpn. J. Med. Sci. Biol. 28*, 73–75.
Johnson, H. M., Bukovic, J. A., & Kauffman, P. E. (1972) *Infect. Immun. 5*, 645–647.
Lehrer, S. S. (1971) *Biochemistry 10*, 3254–3267.
Longworth, J. W. (1971) in *Excited States of Proteins and Nucleic Acids* (Steiner, R. F., & Weinryb, I., Eds.) pp 319–484, Plenum, New York.
Middlebrook, J. L., Spero, L., & Argos, P. (1980) *Biochim. Biophys. Acta 621*, 233–240.
Saxena, V. P., & Wetlaufer, D. B. (1971) *Proc. Natl. Acad. Sci. U.S.A. 68*, 969–972.
Schantz, E. J., Roessler, W. G., Wagman, J., Spero, L., Dunnery, D. A., & Bergdoll, M. S. (1965) *Biochemistry 4*, 1011–1016.
Schmidt, J. J., & Spero, L. (1983) *J. Biol. Chem. 258*, 6300–6306.
Singh, B. R., Kokan-Moore, N. P., & Bergdoll, M. S. (1988) *Biochemistry* (preceding paper in this issue).
Spero, L. (1981) *Biochim. Biophys. Acta 671*, 193–201.
Spero, L., & Morlock, B. A. (1978) *J. Biol. Chem. 253*, 8787–8791.
Spero, L., & Morlock, B. A. (1979) *J. Immunol. 122*, 1285–1289.
Spero, L., Morlock, B. A., & Metzger, J. F. (1978) *J. Immunol. 120*, 86–89.
Stern, O., & Volmer, M. (1919) *Phys. Z. 20*, 183–188.
Teale, F. W., & Weber, G. (1957) *Biochem. J. 65*, 476–482.
Thompson, N. E., Ketterhagen, M. J., & Bergdoll, M. S. (1984) *Infect. Immun. 45*, 281–285.

Photolabeling of Membrane-Bound *Torpedo* Nicotinic Acetylcholine Receptor with the Hydrophobic Probe 3-Trifluoromethyl-3-(*m*-[^{125}I]iodophenyl)diazirine†

Benjamin H. White and Jonathan B. Cohen*
Department of Anatomy and Neurobiology, Washington University School of Medicine, St. Louis, Missouri 63110
Received May 10, 1988; Revised Manuscript Received July 20, 1988

ABSTRACT: The hydrophobic, photoactivatable probe 3-trifluoromethyl-3-(*m*-[^{125}I]iodophenyl)diazirine ([^{125}I]TID) was used to label acetylcholine receptor rich membranes purified from *Torpedo californica* electric organ. All four subunits of the acetylcholine receptor (AChR) were found to incorporate label, with the γ-subunit incorporating approximately 4 times as much as each of the other subunits. Carbamylcholine, an agonist, and histrionicotoxin, a noncompetitive antagonist, both strongly inhibited labeling of all AChR subunits in a specific and dose-dependent manner. In contrast, the competitive antagonist α-bungarotoxin and the noncompetitive antagonist phencyclidine had only modest effects on [^{125}I]TID labeling of the AChR. The regions of the AChR α-subunit that incorporate [^{125}I]TID were mapped by *Staphylococcus aureus* V8 protease digestion. The carbamylcholine-sensitive site of labeling was localized to a 20-kDa V8 cleavage fragment that begins at Ser-173 and is of sufficient length to contain the three hydrophobic regions M1, M2, and M3. A 10-kDa fragment beginning at Asn-339 and containing the hydrophobic region M4 also incorporated [^{125}I]TID but in a carbamylcholine-insensitive manner. Two further cleavage fragments, which together span about one-third of the α-subunit amino terminus, incorporated no detectable [^{125}I]TID. The mapping results place constraints on suggested models of AChR subunit topology.

The nicotinic acetylcholine receptor (AChR)[1] is an integral membrane protein with subunit stoichiometry $\alpha_2\beta\gamma\delta$. Each of the AChR subunits is known to span the membrane, and each is thought to contribute structurally to the AChR ion channel which opens in response to the binding of cholinergic agonists [reviewed by Popot and Changeux (1984), Hucho (1986), and McCarthy et al. (1986)]. The binding sites for agonists and competitive antagonists have been localized to the α-subunits by use of affinity labels (Kao et al., 1984; Pedersen et al., 1986; Dennis et al., 1988), while a high-affinity binding site for noncompetitive antagonists is thought to be formed by all subunits and may be located in the channel itself [reviewed by Changeux and Revah (1987)].

The amino acid sequences of all four subunits are known for the AChR of *Torpedo californica* electric tissue (Noda

† This research was supported in part by USPHS Grants NS 19522 and NS 22828 (Senator Jacob Javits Center for Excellence in Neuroscience). B.H.W. was supported by a National Science Foundation Graduate Fellowship.

[1] Abbreviations: AChR, nicotinic acetylcholine receptor; 43K protein, the basic, membrane-bound 43-kDa protein of *Torpedo* postsynaptic membranes; BSA, bovine serum albumin; α-BgTx, α-bungarotoxin; H_{10}-HTX, *d,l*-decahydro(pentenyl)histrionicotoxin; LIS, lithium diiodosalicylate; SDS, sodium dodecyl sulfate; PAGE, polyacrylamide gel electrophoresis; [^{125}I]TID, 3-trifluoromethyl-3-(*m*-[^{125}I]iodophenyl)diazirine; TPS, *Torpedo* physiological saline (250 mM NaCl, 3 mM $CaCl_2$, 2 mM $MgCl_2$, 5 mM sodium phosphate, pH 7.0); V8 protease, *Staphylococcus aureus* V8 protease.

0006-2960/88/0427-8741$01.50/0